Theory of the spin polarization of field-emitted electrons from nickel

J.-N. Chazalviel* and Y. Yafet
Bell Laboratories, Murray Hill, New Jersey 07974
(Received 13 August 1976)

We calculate the spin polarization of field-emitted electrons from nickel in the framework of the Stoner-Wohlfarth-Slater theory of band magnetism. As was first proposed by Hertz and Aoi for the case of tunneling, we find that the s-d hybridization plays an important role and we give a more quantitative treatment of this effect. The crystal wave functions are described as linear combinations of plane waves and tight-binding d wave functions. In a first approximation the contribution of the d states to the emitted current is neglected; the problem of the matching of the wave functions at the crystal boundary can then be solved exactly and, using the band parameters of Zornberg, very large positive spin polarizations are obtained. Next, the contribution of the d electrons is included in a semiphenomenological way and reasonable agreement with experiment is obtained without invoking any many-body effects. The dependence of the spin polarization on crystallographic direction is investigated. This makes it necessary to consider the case of high-index directions for which field emission may be dominated by surface scattering. The final results compare well with the preliminary measurements of Campagna *et al.*

I. INTRODUCTION

The observation of positive (= majority) electron spin polarizations in photoemission[1] and tunneling experiments[2] from $3d$ ferromagnetic metals generated interest because the results seemed to challenge the Stoner-Wohlfarth-Slater theory of band magnetism.[3] Many-body effects were invoked to account for these positive spin polarizations.[4] Later, Hertz and Aoi[5] pointed out that in the case of tunneling the simple one-electron s-d hybridization in the Bloch functions can also modify the theoretical result in the same direction as do many-body effects. However, the first field-emission measurements[6] had yielded spin polarizations which were very different from those obtained in tunneling. These conflicting results were of little encouragement for producing a real quantitative theory. Recently, Campagna *et al.*[7] started field-emission studies on nickel using a new apparatus; their preliminary results are compatible with those of the tunneling experiments and show that those of Ref. 6 cannot be reliable. These new measurements, done for various known crystallographic directions, are the motivation of the present theoretical investigation.

We deliberately remain in the framework of a one-electron theory. Even so, we are faced with the difficult problem of field emission from Bloch states. We first take a simplified approach (Secs. II and III), neglecting the contribution of d states to the emitted current; this oversimplified picture contains nonetheless the essential features and provides a physical understanding of the effect: In Sec. II the free-electron theory of field emission is recalled, then extended to general band structures, and applied to a nearly-free-electron model; the case of nickel is studied in Sec. III. The consideration of various crystallographic directions makes it necessary to take into account surface scattering which can play an important role for nonsimple orientations; this is considered in Sec. IV. In Sec. V the contribution of d states is introduced in a semiphenomenological manner and the results are discussed in connection with experiment.

II. FIELD EMISSION THEORY

A. Free-electron field emission

We adopt the classical step-potential model for the metal.[8] The extra potential brought by the electric field is given the simple form $-eFz$ ($F, e > 0$). The image potential is neglected. The starting point of the theory is the problem of an electron striking the surface from inside the metal; under the simplifying assumption of a free-electron-like metal, the Hamiltonian is invariant for any translation parallel to the surface plane, and the wave function in the stationary state can be written

$$\Psi = e^{i\vec{k}\cdot\vec{r}} + \zeta e^{i\vec{k}'\cdot\vec{r}} \quad \text{(crystal)}, \qquad \Psi = e^{i\vec{k}_{\parallel}\cdot\vec{r}} g(z) \quad \text{(vacuum)}, \tag{1}$$

where $\vec{k}_{\parallel}$ and k_z are, respectively, the parallel and normal components of $\vec{k}$ relative to the surface; and $\vec{k}' = \vec{k} - 2\vec{k}_z$. In the expression of Ψ, $e^{i\vec{k}\cdot\vec{r}}$ is the incident wave, $\zeta e^{i\vec{k}'\cdot\vec{r}}$ is a reflected wave inside the metal, and $g(z)$ is an evanescent wave in the barrier region. When the evanescent wave reaches the classical turning point A (see Fig. 1), it breaks into two components: an evanescent wave in the $-z$ direction and an outgoing wave in the $+z$ direction. If the electric field is weak $g(z)$ can be derived by using WKB approximation. The result is

$$g(z)=\begin{cases}\xi e^{-(2/3)\kappa z_A}\left[e^{(2/3)\kappa(z_A-z)^{3/2}/z_A^{1/2}}+\dfrac{i}{2}\,e^{-(2/3)\kappa(z_A-z)^{3/2}/z_A^{1/2}}\right]\left(\dfrac{z_A}{z_A-z}\right)^{1/4} & \text{for } z<z_A,\\ \xi e^{-(2/3)\kappa z_A}\dfrac{i-1}{\sqrt{2}}\;e^{(2/3)i\kappa(z-z_A)^{3/2}/z_A^{1/2}}\left(\dfrac{z_A}{z-z_A}\right)^{1/4} & \text{for } z>z_A,\end{cases}$$

with $\kappa^2=2m(\Phi+E_F-E)/\hbar^2+\vec{k}_\parallel^2$; z_A is the abscissa of point A, i.e., $z_A=(\Phi+E_F-E+\hbar\vec{k}_\parallel^2/2m)/eF$, and ξ is a dimensionless parameter. The electrical current density carried by the outgoing wave is

$$\delta j(\vec{k})=-\frac{e}{m}\langle\Psi|p_z|\Psi\rangle$$

$$=-\frac{\hbar e\kappa}{m}\,|\xi|^2e^{-(4/3)\kappa z_A}. \tag{2}$$

Now we are left with the matching of the wave functions at the surface, which must determine the value of ξ and hence $\delta j(\vec{k})$. The continuity of Ψ and $\partial\Psi/\partial z$ is required; these conditions involve $g(0)$ and $dg/dz(0)$, which generally depend on E through z_A. The calculation is greatly simplified if we assume that the electric field is small; in this case $\kappa z_A\gg1$ and the evanescent wave in the $-z$ direction generated at A is negligibly small at 0; the quantities $g(0)$ and $dg/dz(0)$ reduce to ξ and $-\kappa\xi$, respectively, which no longer depend on the applied electric field. This point must be stressed, since it allows to *consider separately* the problem in the vacuum region, which depends *only on the electric field*, and the problem of ξ, which now depends *only on the intrinsic properties of the metal. This parameter ξ characterizes the tailing of the metal wave functions in the vacuum region*; it may depend critically on the nature of these wave functions and its discussion is the main subject of the following sections.

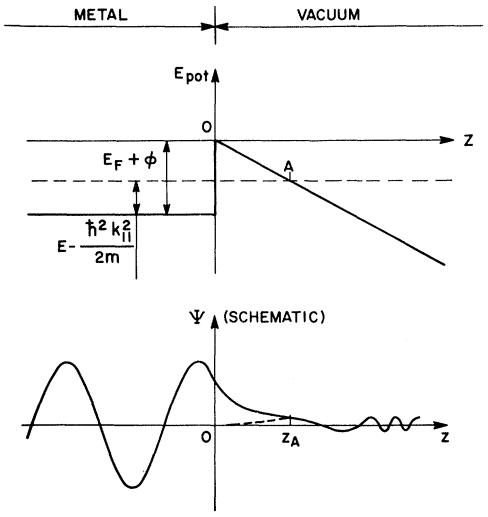

FIG. 1. Schematics of the potential energy and wave function at the metal boundary.

In the case of the free-electron wave functions, the matching is straightforward and gives

$$\xi=1+\zeta=2ik_z/(ik_z-\kappa). \tag{3}$$

The emitted current contributed by electron $|\vec{k}\rangle$ $(k_z>0)$ is then

$$\delta j(\vec{k})=-\frac{\hbar e\kappa}{m}\,\frac{4k_z^2}{k_z^2+\kappa^2}\,e^{-(4/3)\kappa z_A}. \tag{4}$$

The total current is obtained by summing the contributions from all the electrons inside the crystal and with positive k_z. We assume $T=0$. The summation may be written in a convenient way as follows:

$$j=\frac{2}{(2\pi)^3}\int_0^{k_F}dk_z\int_0^{(k_F^2-k_z^2)^{1/2}}\delta j(k_z,k_\parallel)2\pi k_\parallel dk_\parallel.$$

Because of the exponential factor in $\delta j(\vec{k})$ and our assumption of small electric field, the main contribution to j arises from the $|\vec{k}\rangle$ states for which $\kappa^2=\vec{k}_\parallel^2+2m(\Phi+E_F-E)/\hbar^2$ is minimum, $\equiv\kappa_0^2$, that is the electrons close to the Fermi energy and with momentum nearly normal to the surface; a well-known result indeed. This simplifies the calculation of the above integral since one can take $\kappa\approx\kappa_0$:

$$j\approx-\frac{\hbar e\kappa_0}{m}\,\frac{2}{(2\pi)^3}\,e^{-(4/3)\kappa_0\Phi/eF}\,\frac{4k_F^2}{k_F^2+\kappa_0^2}$$

$$\times\int_0^{k_F}\exp\left(\frac{-2\kappa_0(E_F-E)}{eF}\right)dk_z$$

$$\times\int_0^{\infty}\exp\left(\frac{-\kappa_0\hbar^2k_\parallel^2}{meF}\right)2\pi k_\parallel\,dk_\parallel. \tag{5}$$

This gives the well-known Fowler-Nordheim result[8,9]:

$$j=\frac{-e^3F^2}{4\pi^2\hbar\Phi}\,\frac{\kappa_0k_F}{k_F^2+\kappa_0^2}\,e^{-(4/3)\kappa_0\Phi/eF}$$

with

$$\kappa_0^2=2m\Phi/\hbar^2. \tag{6}$$

B. Extension to the general case

Equation (6) holds only for a free-electron-like metal. However, our formulation is readily applicable to a general band structure.

When the wave functions in the metal are Bloch-

like, the tail in the vacuum is no longer expected to have the simple form $\xi e^{i\vec{k}_{\parallel}\cdot\vec{r}}e^{-\kappa z}$. Namely, in the plane $z=0$ one expects strong oscillations with the surface-lattice periodicity:

$$\Psi(z=0)=\sum_{\vec{G}}\xi_{\vec{G}}\,e^{i(\vec{k}_{\parallel}+\vec{G})\cdot\vec{r}}, \tag{7}$$

where the $\vec{G}$'s are vectors of the two-dimensional reciprocal lattice of the surface. From this the behavior of Ψ for $z>0$ is determined by the Schrödinger equation in vacuum

$$\Psi(z>0)=\sum_{\vec{G}}\xi_{\vec{G}}\,e^{(\vec{k}_{\parallel}+\vec{G})\cdot\vec{r}}e^{-\kappa_{\vec{G}}z}, \tag{8}$$

with

$$\kappa_{\vec{G}}^2=\frac{2m}{\hbar^2}(\Phi+E_F-E)+(\vec{k}_{\parallel}+\vec{G})^2. \tag{9}$$

If the surface is a low-index crystallographic plane, $\vec{G}$ is typically of order $2\pi/a$ and at a distance of the surface much larger than a, only the component with $\vec{k}'_{\parallel}=\vec{k}_{\parallel}+\vec{G}\approx 0$ remains. This condition is fulfilled at a finite number of points on the Fermi surface, for example along the z axis ($\vec{G}=0$, $\vec{k}_{\parallel}\approx 0$).

The summation over all the electrons in the crystal can be performed with the same approximations as in Eq. (5), leading to the result

$$j=-\frac{\hbar e\kappa_0}{m}\frac{2}{(2\pi)^3}e^{-(4/3)\kappa_0\Phi/eF}\times\sum_n|\xi|_n^2\int_{(n)}e^{-2\kappa_0(E_F-E)/eF}dk_z\times\int_0^{\infty}e^{-\kappa_0\hbar^2k'^2_{\parallel}/meF}2\pi k'_{\parallel}\,dk'_{\parallel}. \tag{10}$$

Where the index n refers to the various locations on the Fermi surface where the conditions $\vec{k}_{\parallel}+\vec{G}\approx 0$, $v_z>0$ are fulfilled, $E\equiv E(k_z,n)$, and the summation over k_z is over the corresponding region where $E\lesssim E_F$. This latter integral can be rewritten

$$\int_{(n)}e^{-A(E_F-E)}dk_z\approx\frac{1}{|\partial E/\partial k_z|_n}\int_{-\infty}^{E_F}e^{-A(E_F-E)}dE=\frac{1}{A\,|\partial E/\partial k_z|_n}.$$

The final result for j is

$$j=-\frac{e^3F^2}{8\pi^2\hbar^2\kappa_0}e^{-(4/3)\kappa_0\Phi/eF}\sum_n|\xi|_n^2\frac{1}{|v_z|_n}. \tag{11}$$

A comparison with Eq. (6) shows the origin of the factor k_F in that expression. It arises from the product of k_F^2 [in $|\xi|_0^2=4k_F^2/(\kappa_0^2+k_F^2)$] with $1/|v_z|$ ($\propto 1/k_F$). Its proportionality to the three-dimensional density of states is purely fortuitous. In fact if ξ were evaluated from the WKB approximation instead of the sharp-boundary model, one would get $|\xi|_0^2=k_F/\kappa_0$ and the final j would no longer depend on k_F, a result which was pointed out by Harrison.[10] The meaningful density of states here is one dimensional,[8] and corresponds to the factor $1/|v_z|$.

In conclusion and as is seen from Eq. (11), the total current in the low-electric-field limit depends on the band structure only through the factor $\sum_n|\xi^2/v_z|_n$ and in the following we focus our interest on this factor.

C. Nearly-free-electron band structure

We consider field emission from a low-index crystallographic face, in which case the points of interest on the Fermi surface [referred to as n in Eq. (11)] are its intersections with Oz. We assume that the Fermi energy falls into the lowest nearly-free-electron band, as shown in Fig. 2. Then there are only two such intersections and we are interested only in that with $k_z>0$. The wave function at this point of the Brillouin zone is of the form

$$\Psi_{k_z}=u_0e^{ik_zz}+u_1e^{i(k_z-2k_M)z},$$

where k_M is the value of k_z at the zone boundary, and u_0 and u_1 are functions of k_z. The reflected wave function is of the form $\xi\Psi_{-k_z}$. The problem turns out to be pseudo-one-dimensional and the matching at the crystal face can be performed with an evanescent wave $\xi e^{-\kappa z}$, just as in the free-electron model. If the origin is chosen on the last plane of atoms, u_0 and u_1 can both be taken to be

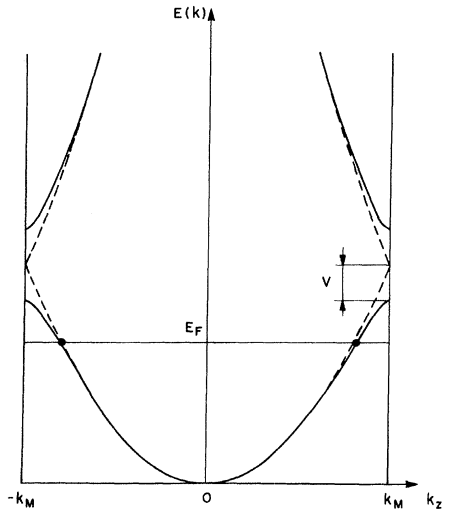

FIG. 2. Band structure along the k_z direction in our nearly-free-electron model.

real, for example, $u_0 = \cos\varphi$; $u_1 = \sin\varphi$, and then $\tan 2\varphi = -V/E_0$, where V is the component of the pseudopotential at $2\vec{k}_M$, and $E_0 = \hbar^2(k_z^2 - k_M^2)/2m$. The sharp boundary is assumed to lie at a distance d of the last atomic plane, and we define $\theta = 2k_M d$. Then performing the matching yields

$$\xi = [2ik_M \cos 2\varphi + 2i(k_z - k_M)(1 + \sin 2\varphi \cos\theta)] \times [(ik_z - \kappa)\cos\varphi + (ik_z - \kappa - 2ik_M)\sin\varphi e^{i\theta}]^{-1}. \tag{12}$$

This expression can be simplified if the pseudopotential V is small. In this case, φ is vanishingly small unless $k_z \approx k_M$. In the regime $k_z \neq k_M$, $\varphi = 0$, we recover the free-electron result [Eq. (3)]. Near the zone boundary, φ can be appreciable, but then we can let $k_z = k_M$ in Eq. (12), which gives

$$|\xi|^2 \approx \frac{4k_M^2 \cos^2 2\varphi}{k_M^2 + \kappa^2 - \sin 2\varphi [k_M^2 \cos\theta - \kappa^2 \cos\theta + 2\kappa k_M \sin\theta]}. \tag{13}$$

The behavior of $|\xi|^2$ is dominated by the term $\cos^2 2\varphi$ in the numerator of Eq. (13). This can be rewritten $\cos^2 2\varphi = E_0^2/(E_0^2 + V^2)$, where $E_0 = \hbar^2(k_z^2 - k_M^2)/2m$ vanishes at the zone boundary. The essential effect of this term is therefore to introduce a cutoff in $|\xi|^2$ as compared to the free-electron result. The term in square brackets in the denominator depends on the choice of the position of the sharp boundary; this term does not affect the qualitative behavior of $|\xi|^2$, but may introduce some change in the absolute magnitude near the zone boundary.[11] We ignore it in the following for simplicity: the errors involved in the case of nickel are thought to be small and anyway they are confined to very few regions in $\vec{k}$ space where the Fermi surface approaches the zone boundary. With this approximation, we get the very simple result

$$|\xi|^2 \approx [4k_z^2/(k_z^2 + \kappa^2)]\cos^2 2\varphi. \tag{14}$$

The quantity of interest for field emission is $|\xi^2/v_z|$ (see Fig. 3), which comes out straightforwardly by noting that $v_z = \cos 2\varphi \hbar k_z/m = v_z^0 \cos 2\varphi$, hence

$$\left|\frac{\xi^2}{v_z}\right| = \frac{4k_z^2}{k_z^2 + \kappa^2}\frac{m}{\hbar k_z}\cos 2\varphi = \frac{|\xi_0|^2}{|v_z^0|}(u_0^2 - u_1^2). \tag{15}$$

The rapid decrease of the current as k_z approaches the zone boundary is illustrated in Fig. 3.

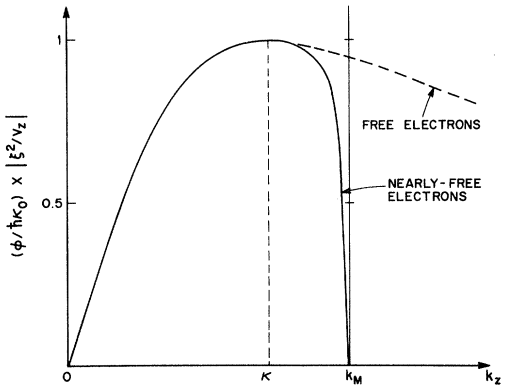

FIG. 3. Plot of $|\xi^2/v_z|$ (in units of $\hbar\kappa_0/\Phi$) the quantity which governs the field emitted current vs the Fermi wave vector. The dashed line is the free-electron case; the solid line is for our nearly-free-electron model.

III. FIELD EMISSION FROM NICKEL

The band structure of nickel has been calculated and accurately fitted with the *combined-interpolation scheme*.[12,13] This model approximates the Bloch functions by linear combinations of tight-binding $3d$ wave functions and orthogonalized plane waves.[14] Such a description is directly usable in our simple theory of field emission. In this section, we assume that the $3d$ wave functions are very localized and play no role in field emission. Some support for this assumption is given by the estimates of Politzer and Cutler, and of Gadzuk, which give a tunneling probability for the d states about 10^{-3} to 10^{-1} times that for free electrons.[15] This is in agreement with experimental observations.[16] See also the simplified argument given in the Appendix. Nevertheless, neglecting completely the d-tunneling contribution is a poor approximation because of the large d density of states at the Fermi level: This will be discussed in Sec. V.

The wave functions as taken by Zornberg[13] are of the form

$$\Psi_{\vec{k}} = \sum_{i=0}^{3} u_i \varphi_{\vec{g}_i}^{\mathrm{OPW}}(\vec{r}) + \sum_n \sum_{j=1}^{5} v_j d_j(\vec{r} - \vec{R}_n) e^{i\vec{k}\cdot\vec{R}_n}, \tag{16}$$

where the d_j's are the nickel $3d$ atomic wave functions, the $\vec{R}_n$'s are the positions of the lattice sites, and $\varphi_{\vec{g}_i}^{\mathrm{OPW}}$ is obtained from the plane wave $\exp[i(\vec{k} + \vec{g}_i)\cdot\vec{r}]$ by orthogonalization to the d wave functions. Here $\vec{g}_i$ is a vector of the reciprocal lattice (including $0 = \vec{g}_0$). Four such orthogonalized plane waves (OPW) are sufficient for a good representation of the wave functions in the reduced Brillouin zone ($\frac{1}{48}$th of the initial Brillouin zone).

If the d functions are assumed very localized, the matching at the crystal surface is governed by the OPW part of $\Psi_{\vec{k}}$; this fits directly into our nearly-free-electron model. The value of the tailing parameter ξ is, from Eq. (14),

$$|\xi|^2 = \frac{4k_z^2}{k_z^2+\kappa^2} \times\left[|u_0|^2 - (|u_1|^2+|u_2|^2+|u_3|^2)\right]\Big/\left(\sum_i |u_i|^2\right)\Big]^2 \times\sum_i |u_i|^2 . \quad (17)$$

The second factor in Eq. (17) is the same as the cutoff factor in Eq. (14). Far from the zone edge, u_0 is much larger than the other u_i's, and this reduces to unity; near a face of the zone, two among the four OPW's become equivalent, and the factor vanishes. The last factor $\sum_i |u_i|^2 = u^2$ has been introduced into Eq. (17) to take care of the hybridized nature of the wave functions: the wave functions are normalized

$$\left(\sum_i |u_i|^2 + \sum_j |v_j|^2 = u^2 + v^2 = 1\right),$$

but only the OPW part is assumed to contribute to the emitted current.

At this point a look at the band structure (see Fig. 4) shows the kinds of effect that we can expect. The narrow d bands and the free-electron paraboloid do not cross but are strongly hybridized, especially in the vicinity of the Fermi energy. As is seen from Eq. (17), this hybridization

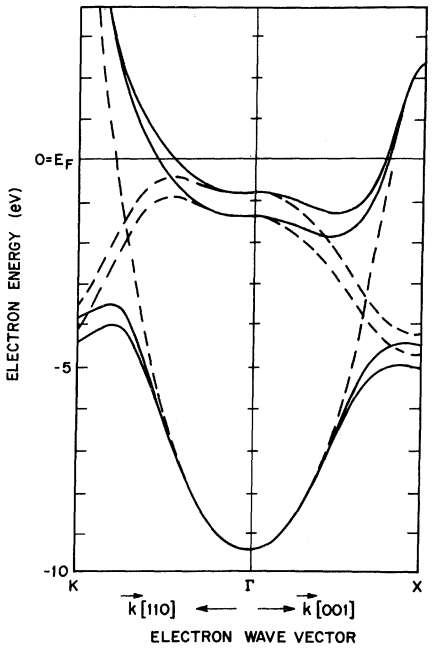

FIG. 4. Simplified band structure of nickel along [100] and [110] directions. The dashed lines would correspond to the bands in the absence of hybridization. The eight unhybridized d bands have been omitted for clarity.

is expected to modify $|\xi^2/v_z|$, which is the relevant quantity for field emission. Since the spin-up and spin-down $3d$ subbands lie at different energies in ferromagnetic nickel, the hybridization at the Fermi level is different for up- and down-spin electrons, and even if only the OPW part is considered, the field-emitted current will be different for the two. Such an idea was first proposed by Hertz and Aoi.[5] The present treatment is however essentially different from theirs: Their approach is a tight-binding calculation of the tunneling through an oxide layer and the "s" and d states are treated on equal grounds as tight-binding wave functions, which may be bad for the "s" states. Here the plane-wave part (instead of "s") is treated as in the Fowler-Nordheim theory, which, we believe, is a more appropriate way at least for field emission. This is realized at the cost of a worse approximation for the d contribution (to be discussed in Sec. V).

The hybridization affects the ratio $|\xi^2/v_z|$ in different ways: the hybridized form of the wave function enters directly $|\xi|^2$ via the factor u^2, and the shape of the energy bands introduces changes in $|v_z|$ and in $|\xi|^2$ via the factor $k_z^2/(k_z^2+\kappa^2)$. This last factor has no analogy in the treatment of Ref. 5.

Elementary mechanism: An idealized model

Before going into a numerical calculation of these effects for nickel, it is helpful for the physical understanding to consider a simplified model of the s-d hybridization. The d bands are assumed to be flat and the s band rectilinear ($E_s = ak_z$ in the z direction) which is always possible in a small energy interval and with a suitable origin. We allow hybridization between the s and d_z bands by introducing a nondiagonal matrix element $H_{sd_z} = V$ in the crystal Hamiltonian. The resulting hybridized bands are of the form (see Fig. 5)

$$E_1 = \tfrac{1}{2}(E_s+E_d) + \tfrac{1}{2}[(E_s-E_d)^2+4V^2]^{1/2},$$
$$E_2 = \tfrac{1}{2}(E_s+E_d) - \tfrac{1}{2}[(E_s-E_d)^2+4V^2]^{1/2}, \quad (18)$$

and the hybridization factor u^2 in Eq. (17) is $u^2 = (E-E_d)^2/[V^2+(E-E_d)^2]$, where $E = E_1$ or E_2, according to the band under consideration. Let us assume for instance that the Fermi level falls into the upper band E_1. The velocity v_z then follows directly from Eqs. (18),

$$v_z = \frac{1}{2\hbar}\left(1+\frac{E_s-E_d}{[(E_s-E_d)^2+4V^2]^{1/2}}\right)\frac{dE_s}{dk_z} = \frac{a}{\hbar}\,\frac{(E-E_d)^2}{V^2+(E-E_d)^2}. \quad (19)$$

The effect of hybridization on u^2 and on v_z cancels

out in the ratio $|\xi^2/v_z|$. The only term left is the modification of $|\xi|^2$ via the change in k_z. This change is $\Delta k_z = -V^2/[a(E-E_d)] < 0$. Now if we consider separately the up-spin and down-spin electrons, in a ferromagnetic metal $E_{d\uparrow} < E_{d\downarrow}$ and therefore in our model k_z is smaller for minority electrons. This results in a different value of the ratio $|\xi^2/v_z|$ for up- and down-spin electrons, and therefore leads to a spin polarization of the emitted current, *although the tunneling from d states has been completely neglected.* Inspection of the expression of $|\xi|^2$ [Eq. (17)] shows that this polarization *is expected to be positive* (i.e., of the same direction as in the metal).

Numerical calculation: Results

The numerical calculation of $|\xi^2/v_z|$ for up- and down-spin electrons has been done for nickel, starting from the band structure and the parameters of Zornberg[13,17] and taking $\Phi = 5$ eV. This calculation was done for various crystallographic directions, although the use of Eq. (17) should be restricted to low-index crystallographic faces (see Sec. IV B). The results are plotted in Fig. 6 and are in qualitative agreement with the predictions of our idealized model.

In the [001] direction, the amount of hybridization at the Fermi level is small, and the polarization is, as expected, of the order of $(k_{z\uparrow} - k_{z\downarrow})/k_z \sim 10^{-2}$. When one gets slightly off the [001] direction, the s band becomes hybridized with the highest d band (such an hybridization is symmetry forbidden along [001]). The latter is known to be responsible for the down-spin ellipsoidal hole pocket near X. As a result of the hybridization, the s character at the Fermi level for down spins is shared between this hole pocket and the main sheet of the Fermi surface. This does not affect drastic-

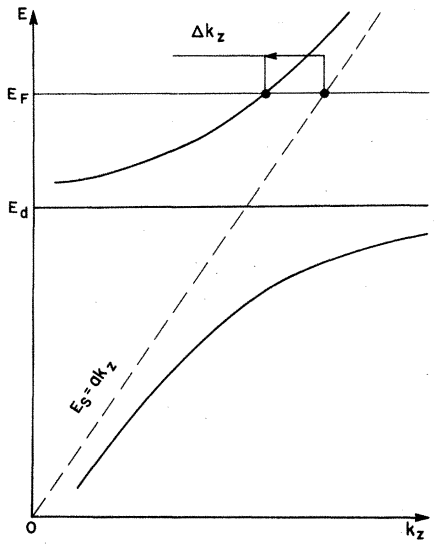

FIG. 5. Our idealized model for s-d hybridization: flat d band and rectilinear s band (see text).

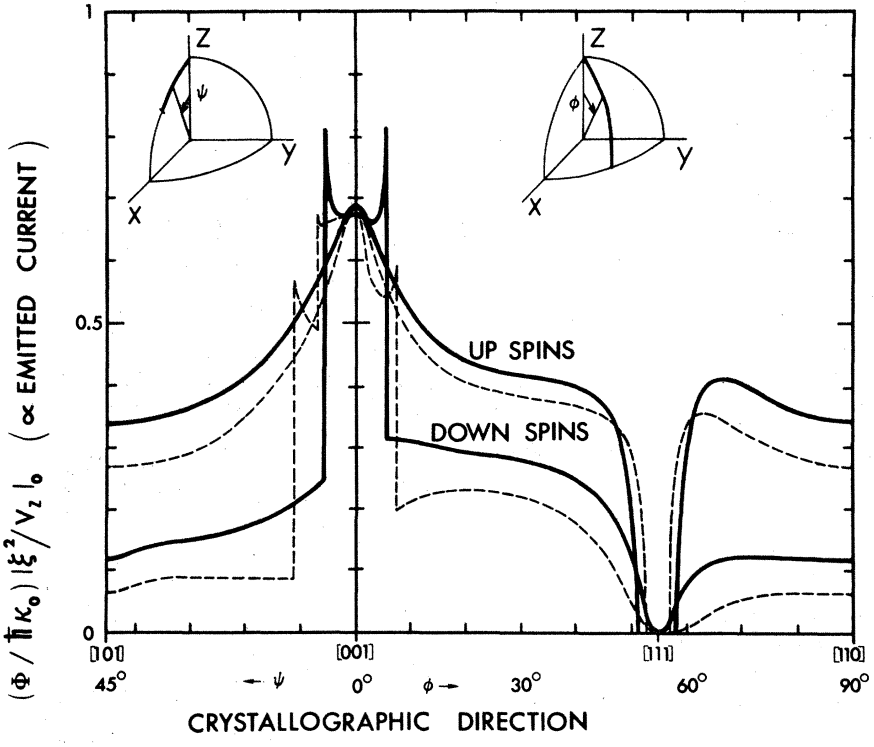

FIG. 6. Results of the numerical calculation for nickel. The plotted dimensionless quantity is directly proportional to the (up-spin or down-spin) emitted current. For free electrons, it would be $2k_F\kappa_0/(k_F^2+\kappa_0^2) \approx 1$ (see Fig. 3). The solid lines are the result of the calculation at the Fermi level. The dashed lines are the result at $E_F - 0.2$ eV (see Sec. IV A).

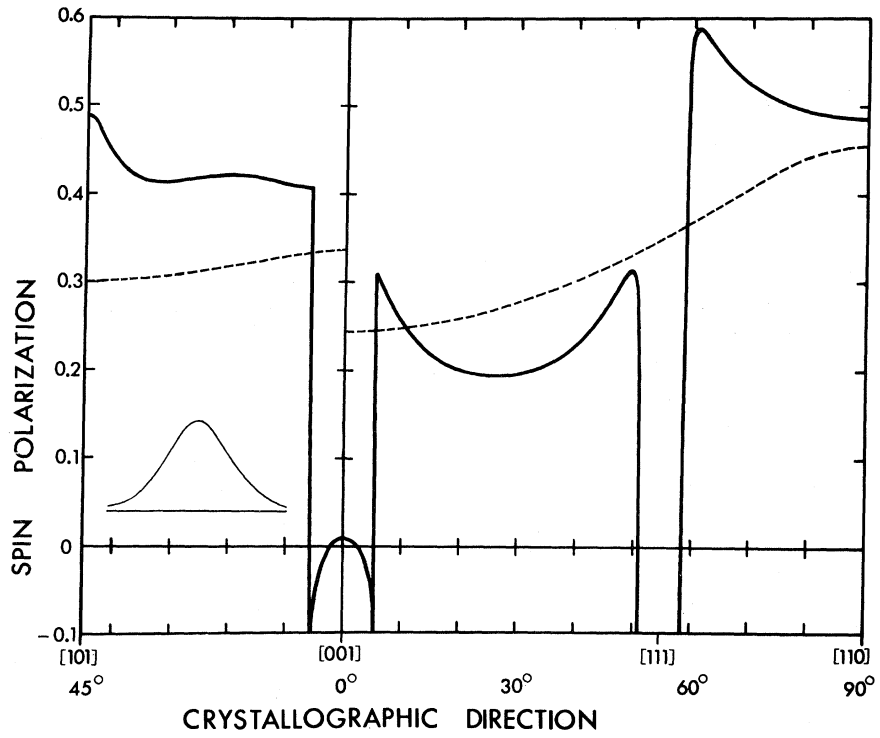

FIG. 7. Plot of the spin polarization as a function of crystallographic direction along $[x01]$ and $[11x]$. The solid line is the main result. The dashed line corresponds to the case of extreme surface scattering (see Sec. IV B). The bell-shaped curve in the lower left-hand corner gives the scale of the averaging which would be involved for the case of a typical electric field (see Sec. IV A).

ally the down-spin current up to a critical angle $\theta_c \approx 5.5°$ off the [001] direction. Beyond this value, the k_z radius vector no longer intersects the ellipsoidal hole pocket. In other words, the lower hybridized band sinks below the Fermi level. Since about half of the s character is carried by this band, there results a sudden decrease of the down-spin current (see Fig. 6). No such change occurs for the up-spin electrons, because the d bands are deeper and the Fermi surface has a single sheet.

In the [110] direction, the calculated spin polarization is 0.5. This is still larger than the expected value from the idealized model $p \approx (k_{z\uparrow} - k_{z\downarrow})/k_z = 0.2$; this deviation comes from the curvature of the bands and the strong dependence of V upon k_z.[14] In the [111] direction, both the up-spin and down-spin currents vanish identically, because the k_z radius vector has no intersection with the up-spin Fermi surface, and the intersection with the down-spin Fermi surface is purely d character.

IV. SPIN-POLARIZATION: DISCUSSION OF RESULTS

The spin polarization $p = (j\uparrow - j\downarrow)/(j\uparrow + j\downarrow)$ is plotted as the solid line in Fig. 7 for the $[x01]$ and $[11x]$ directions. Figure 8 maps p for all the crystallographic directions. A most interesting feature of Fig. 8 is the lower value of the polarization along the directions between [001] and [111], this is in qualitative agreement with experiment, since negative spin polarizations have been observed in this region. From a quantitative point

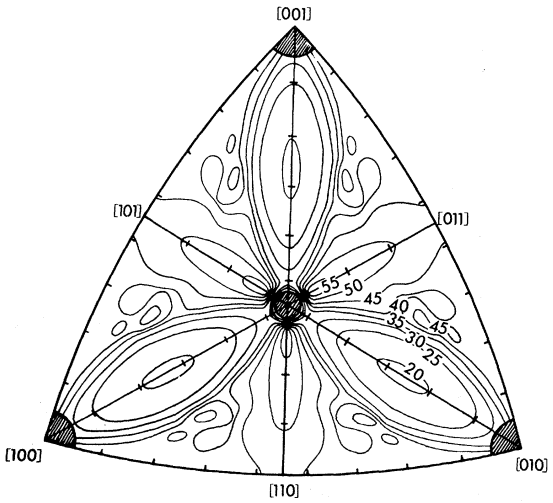

FIG. 8. Spin polarization as a function of crystallographic orientation. This is a stereographic projection around [111]. The lines correspond to constant polarizations from 20% to 55% by increments of 5%. The hatched areas correspond to $p < 20\%$. Note the valleys between [001] and [111]. Most of the sharp features like the wells near [001] and [111], would be smeared out by the effect of a finite electric field and surface scattering.

of view, the calculated polarizations differ from the experimental ones in two respects: first *the very large values* (typically 20% to 60%, as compared with the experimental −3% to +10%)[7,2,18]; this is an obvious consequence of our neglect of d tunneling and will be discussed in Sec. V; second the *sharp variations and discontinuities* of p in the vicinity of [001] and [111]; these unphysical features are removed, in practice, by two effects, which we discuss briefly: the effect of a finite electric field and surface scattering.

A. Effect of a finite electric field

The above calculation was based on Eq. (11), which is valid only for vanishingly small electric field. It can be shown from Eq. (10) that the essential effect of a non-null electric field is to replace $|\xi^2/v_z|_n$ in Eq. (11) by its average value in a small volume of the Brillouin zone, defined by $E_F - E \lesssim eF/2\kappa_0$ and $k_{\parallel}^2 \lesssim meF/\kappa_0\hbar^2$. For a typical electric field $F \approx 5\times 10^7$ V/cm this gives $E_F - E \lesssim 0.2$ eV and $k_{\parallel} \lesssim 0.2$ Å^{-1}. The effect of the averaging over E has been estimated by calculating $\sum_n |\xi^2/v_z|_n$ at the energy $E_F - 0.2$ eV. The resulting currents, shown as the dashed lines in Fig. 6, are rather similar to the results at E_F, and therefore the averaging over E should play no essential role. In contrast, the averaging over $k_{\parallel}$ would yield a smoothing of the curves in Fig. 6; this would spread out the discontinuities over a typical angle $\Delta k_{\parallel}/k_z \sim 0.2$ Å$^{-1}/1$ Å$^{-1} \approx 10°$. This is quite an appreciable angle (see the bell-shaped curve in Fig. 7) and therefore most of the sharp features in Figs. 6–8 should not be observed experimentally.

B. Effect of surface scattering

Equation (11) has been derived for simple crystallographic directions, such that the condition $\vec{k}_{\parallel} + \vec{G} = 0$ is fulfilled only for $\vec{k}_{\parallel} = \vec{G} = 0$. Using Eq. (11) for every direction, as we have done, is therefore somewhat unjustified. It is shown elsewhere[11] that field emission from high-index planes can be treated with a scattering formalism; the essential result is the addition of a "scattered" current j' to the "specular" current j of Eq. (11). For the directions [11x] and [x01] in nickel, the scattering potentials are due to atomic steps parallel to [1$\bar{1}$0] and [010] respectively. As shown in Ref. 11, the scattered current j' in this case is given by

$$j'_{\text{step}} = -\frac{e^3F^2}{8\pi^2\hbar^2\kappa_0}\left(\frac{m}{\hbar^2}\right)^2\frac{d_s}{\kappa_0} \times\left[\int |V'_{\vec{k}_0\vec{k}_F(\theta)}|^2\frac{k_F(\theta)}{\kappa_0}\frac{1}{|v_F(\theta)|}\frac{d\theta}{2\pi}\right] \times e^{-(4/3)\kappa_0\Phi/eF}, \tag{20}$$

where θ is the polar angle of the $\vec{k}$ vector in the plane perpendicular to the direction of the steps and summation is limited to the regions where $v_z > 0$, $v_F(\theta)$ is the radial component of the Fermi velocity, d_s is the density of steps for unit length, $\vec{k}_0$ is the Fermi wave vector normal to the surface, and $V'_{\vec{k}_0\vec{k}_F(\theta)}$ is the matrix element of the two-dimensional scattering potential (the potential produced by an atomic step is translation invariant along the third dimension, i.e., the step direction). The scattered current j' is expected to be of the same order of magnitude as j, except when d_s is accidentally small (i.e., near [100], [111], or [110]). It is less sensitive than j to the local properties of the Fermi surface, because the integral in Eq. (20) involves an angular averaging on $\vec{k}$. As an example, we have chosen a localized potential (i.e., range much shorter than $1/k_F$ and $1/\kappa_0$). Then an appropriate expression for the matrix element is[11]

$$V'_{\vec{k}_0\vec{k}_F(\theta)} \approx C(k_0)\xi[\vec{k}_F(\theta)]\int\int V'(\vec{r})\,d^2\vec{r}\,. \tag{21}$$

The strong dependence of ξ upon θ is averaged out by the integral in Eq. (20). The only memory of the local properties of the Fermi surface comes from the dependence of $V'_{\vec{k}_0\vec{k}_F(\theta)}$ on $\vec{k}_0$ [the first factor in Eq. (21)]. This is a fairly weak dependence [$C(k_0) = 2\kappa_0/(\kappa_0 - ik_0)$ for free electrons],[11] although it can be less simple in the case of an arbitrary Fermi surface. If one neglects this factor, one can get an estimate of the maximum possible averaging via the surface-scattering mechanism. The corresponding spin polarization $(j'_{\uparrow} - j'_{\downarrow})/(j'_{\uparrow} + j'_{\downarrow})$ is plotted as the dashed line in Fig. 7. All the sharp features have disappeared, but the general behavior is unchanged; namely, the polarization is still minimum between [001] and [111].

In conclusion, both the finiteness of the electric field and the surface scattering are likely to smear out the discontinuities of the polarization as a function of crystallographic direction, but neither of them are too strong and the essential features seem to be conserved. Our simplified approach of neglecting d tunneling appears therefore successful in that it gives correctly the qualitative behavior of spin polarization as a function of direction. Furthermore, it shows that hybridization can give *very large effects* and explain *positive spin polarizations*. As a consequence, no comparison of many-body theories with experiment seems possible before d tunneling is accurately understood.

V. CONTRIBUTION OF d TUNNELING

The contribution of d tunneling is expected to play a crucial role in view of the large density of

d states at the Fermi level. This should decrease the very large values of the polarization which were obtained above.

The problem of field emission from tight-binding d states has been considered in detail by Gadzuk and by Politzer and Cutler.[15] A simplified argument is given in the Appendix. The conclusion is that their contribution to the field-emitted current (i.e., the $|\xi|^2$ factor), is 10 to 10^3 times smaller than for free electrons. The densities of states at the Fermi level for nickel are in the ratios $\rho_{d\uparrow} \sim \rho_{s\uparrow} + \rho_{s\downarrow} \sim 10^{-1}\rho_{d\downarrow}$ and therefore the contribution of $d\downarrow$ states should not be neglected as compared to s states. A serious (numerical) treatment of field emission from hybridized Bloch functions is beyond the scope of this work and we will content ourselves with a semiphenomenological argument: We assume that the effect of d states is mainly to add a constant down-spin current $J_{d\downarrow}$ independent of the crystallographic orientation. The neglect of the analogous $J_{d\uparrow}$ is probably justified, but the assumed isotropy and the supposed additivity may be somewhat unrealistic. However, taking $J_{d\downarrow}$ as an adjustable parameter, the results of Sec. IV can be brought into reasonable agreement with experiment. Writing

$$J_{d\downarrow} = -e^3F^2/(16\pi^2\hbar\,\Delta E)\exp(-\tfrac{4}{3}\kappa_0\Phi/eF)$$

by analogy with Eq. (6) and taking $\Delta E = \Phi/0.185$ ($\Phi/\Delta E$ is to be compared with the quantity plotted in Fig. 6 for the s part), we get $p([112]-[113]) \approx -5.1\%$ and $p([102]-[103]) \approx +7.2\%$ in typical agreement with the experimental values -2.9% and $+3.6\%$, respectively.[7] The smaller contrast observed experimentally may be a consequence of surface scattering (starting from the scattered currents j'_{step} discussed in Sec. IV B would yield polarizations of -1.0% and $+2.5\%$, respectively). The obtained value of $J_{d\downarrow}$ is roughly $\frac{1}{3}(j_\uparrow + j_\downarrow)$. In view of the ratio of the densities of states $\rho_{d\downarrow} \sim 10(\rho_{s\uparrow} + \rho_{s\downarrow})$, this implies a $|\xi|^2$ factor about 30 times smaller for the d states than for free electrons. This order of magnitude is very much as expected.

VI. CONCLUSION

We have shown that the hybridization in the Bloch functions has an important effect on the spin polarization of the emitted current. By neglecting d tunneling and using a nearly-free-electron model modified to include hybridization, we have obtained very large positive polarizations. The semiphenomenological inclusion of the d contribution as an additive constant down-spin current permits to get agreement with experiment. Although this is not conclusive in regard to the magnitude of the many-body effects, it shows that the right order of magnitude and angular dependence of the spin polarization can be obtained in the framework of a *one-electron theory*. We believe that this simple calculation should stimulate more systematic investigations of this problem by the use of numerical methods.

ACKNOWLEDGMENTS

The authors have enjoyed many invaluable discussions with Dr. M. Campagna and Dr. M. Landolt. They are also indebted to Dr. N. V. Smith for kindly supplying the program of band-structure calculation.

APPENDIX: FIELD EMISSION FROM TIGHT-BINDING STATES: A SIMPLIFIED ARGUMENT

We consider a simple cubic lattice, with nearest-neighbor tight-binding wave functions. We further assume that the basic atomic functions φ have s symmetry. An incident wave can be written

$$\Psi_{\text{inc}} = \sum_n e^{ik_z na} \sum_{p,q} e^{i(k_x p + k_y q)a} \varphi(\vec{r} - \vec{R}_{pqn}),$$

where $\vec{R}_{pqn}$ is the lattice point with coordinates (pa, qa, na). If we superpose a wave

$$\Psi' = -e^{2ik_z a} \sum_n e^{-ik_z na} \sum_{p,q} e^{i(k_x p + k_y q)a} \varphi(\vec{r} - \vec{R}_{pqn}),$$

then the sum vanishes identically on the sites $n = 1$, that is on the atomic plane $z = a$. We now cut the crystal between $z = 0$ and $z = a$, throwing away the part $z \geq a$; this creates a [001] face and one can check that an eigenfunction of the new system is

$$\Psi = \sum_{n \leq 0} (e^{ik_z na} - e^{2ik_z a} e^{-ik_z na}) \times \sum_{p,q} e^{i(k_x p + k_y q)a} \varphi(\vec{r} - \vec{R}_{pqn}). \tag{A1}$$

And so the matching is performed (this trick works only in the nearest-neighbors approximation). For $\vec{k}_{\parallel} = 0$, the tailing parameter ξ can be obtained by summing the tails of each atomic wave function in the crystal. We take the asymptotic behavior $\varphi_{lm}(\vec{r}) \sim \eta Y_{lm}(\theta, \varphi) e^{-\kappa r}/\kappa r$, where φ_{lm} can be now any type of wave function (we forget the problem of hybridization between different d states) and includes a factor such that $\langle \sum_j |\varphi(\vec{r} - \vec{R}_j)|^2 \rangle = 1$ [i.e., $\varphi(\vec{r})$ and η are dimensionless]. Far from the surface into vacuum, the tail is

$$2ie^{ik_z a\eta}\sum_{n=-\infty}^{0}\sin[k_z(n-1)a]\sum_{p,q}Y_{1m}(\theta,\varphi)\frac{\exp(-\kappa|\vec{r}-\vec{R}_{pqn}|)}{\kappa|\vec{r}-\vec{R}_{pqn}|}\approx -ie^{ik_z a\eta}\frac{e^{\kappa a}\sin k_z a}{\cosh\kappa a-\cos k_z a}\frac{2\pi}{\kappa^2 a^2}Y_{10}(\theta=0)\delta_{m0}e^{-\kappa z}. \tag{A2}$$

This has to be identified with $\xi e^{-\kappa(z-z_0)}$, where z_0 is the abscissa of the plane where the electric field Hamiltonian vanishes (in other words, the "electric surface" of the crystal). It gives

$$|\xi|^2=\frac{(2l+1)\pi\eta^2}{(\kappa a)^4}\delta_{m0}e^{-2\kappa z_0}\left(\frac{e^{\kappa a}\sin k_z a}{\cosh\kappa a-\cos k_z a}\right)^2. \tag{A3}$$

The last factor is nearly equal to $4\sin^2 k_z a$ because, in practice, $\cosh\kappa a \gg 1$ (only the last atomic plane contributes to the tail) and is comparable to the $|\xi|^2$ factor for free electrons. The Kronecker δ_{m0} shows that several atomic functions do not contribute to field emission, due to symmetry considerations. Finally, we can get an estimate of the ratios of d to free-electron tunneling [we replace δ_{m0} by $1/(2l+1)$]

$$|\xi|_d^2/|\xi|_{\text{free}}^2\sim[\pi\eta^2/(\kappa a)^4]e^{-2\kappa z_0}. \tag{A4}$$

We have evaluated η for nickel by matching the radial part of the atomic function to the asymptotic form $\eta e^{-\kappa r}/\kappa r$, at a distance from the center equal to the Wigner-Seitz radius 1.37 Å; this gives $\eta\approx 1.2$. For a in the denominator of Eq. (32) we have rather taken $a/\sqrt{2}\approx 2.48$ Å, because for the [100] face of a fcc crystal, the density of atoms per unit area is $2/a^2$ instead of $1/a^2$. From the work function of 5 eV one gets $\kappa\approx 1.15$ Å^{-1}. This gives $|\xi|_d^2/|\xi|_{\text{free}}^2\sim\frac{1}{20}e^{-2\kappa z_0}$. A realistic value for z_0 lies probably in the range 0 to $\frac{1}{4}a$, hence the final estimation

$$\tfrac{1}{150}\lesssim|\xi|_d^2/|\xi|_{\text{free}}^2\lesssim\tfrac{1}{20} \tag{A5}$$

is in order-of-magnitude agreement with other estimates.[15]

*On leave from Laboratoire de Physique de la Matière Condensée, Ecole Polytechnique, 91120 Palaiseau, France.

[1]G. Busch, M. Campagna, and H. C. Siegmann, Phys. Rev. B 4, 746 (1971).
[2]R. Meservey and P. M. Tedrow, Solid State Commun. 11, 333 (1972); Phys. Rev. B 7, 318 (1973).
[3]See, for example, H. C. Siegmann, Phys. Rep. C 17, 37 (1975); and M. Campagna, D. T. Pierce, F. Meier, K. Sattler, and H. C. Siegmann, Adv. Electron. Electron Phys. 41, 113 (1976).
[4]See, for example, P. W. Anderson, Philos. Mag. 24, 203 (1971); W. Baltensperger, Helv. Phys. Acta 45, 203 (1972); S. Doniach, AIP Conf. Proc. 5, 549 (1972).
[5]J. A. Hertz and K. Aoi, Phys. Rev. B 8, 3252 (1973).
[6]W. Gleich, G. Regenfus, and R. Sizmann, Phys. Rev. Lett. 27, 1066 (1971).
[7]M. Campagna, T. Utsumi, and D. N. E. Buchanan, J. Vac. Sci. Technol. 13, 193 (1976); and M. Campagna and M. Landolt (unpublished).
[8]For a comprehensive review on both the theoretical and experimental aspects of field emission, see J. W. Gadzuk and E. W. Plummer, Rev. Mod. Phys. 45, 487 (1973); and R. Gomer, Field Emission and Field Ionization (Harvard U. P., Cambridge, Mass., 1961).
[9]R. H. Fowler and L. Nordheim, Proc. R. Soc. A 119, 173 (1928).
[10]W. A. Harrison, Phys. Rev. 123, 85 (1961).
[11]J.-N. Chazalviel (unpublished).
[12]L. Hodges, H. Ehrenreich, and N. D. Lang, Phys. Rev. 152, 505 (1966).
[13]E. I. Zornberg, Phys. Rev. B 1, 244 (1970).
[14]F. M. Mueller, Phys. Rev. 153, 659 (1967).
[15]B. A. Politzer and P. H. Cutler, Surf. Sci. 22, 277 (1970); and Mat. Res. Bull 5, 703 (1970); J. W. Gadzuk, Phys. Rev. 182, 416 (1969).
[16]M. Campagna and T. Utsumi, AIP Conf. Proc. 24, 399 (1974).
[17]The present calculations are done using the parameter set PS IV of Ref. 13. We have checked that this choice is not critical; using PS VI yields the same spin polarizations with a maximum absolute discrepancy of 0.03.
[18]The polarizations measured by tunneling (7.5% to 10%) are appreciably larger than those so far reported in field emission (−2.9% to +7.4%). The tunneling data are unfortunately difficult to discuss quantitatively, because they are taken from polycrystalline films and must correspond to some average on all the crystallographic directions. The averaging probably favors the directions with lowest Φ, which are the high index planes. From Fig. 8 these directions are seen to give calculated polarizations in the 40%–45% range; the calculation in the case of strong surface scattering also yields an almost constant value $p\approx 43\%$. But the averaging to be performed might as well be dominated by the geometry of the surface, itself determined by thermodynamics: one may speculate that the film tends to form [111] microfacets, in that case the electric field would be concentrated on the "ridges" between two facets, and this would favor the [111] to [1$\bar{1}$1] directions (which would be just the region of highest polarization). Further field-emission investigations should help to clarify these tunneling results.